INSTITUTE FOR FUSION STUDIES

DOE/ET-53088-608 IFSR #608

Profile Stabilization of Tilt Mode in a Field Reversed Configuration

J.W. COBB, T. TAJIMA
Institute for Fusion Studies
The University of Texas at Austin
Austin, Texas 78712
and
D.C. BARNES
Los Alamos National Laboratory
P.O. Box 1663
Los Alamos, New Mexico 87545

June 1993

THE UNIVERSITY OF TEXAS

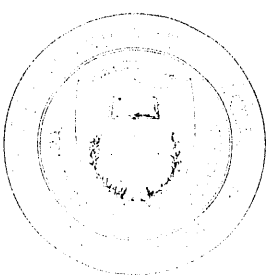

AUSTIN

DISCLAIMER

Profile Stabilization of Tilt Mode in a Field Reversed Configuration

John W. Cobb, T. Tajima
Institute for Fusion Studies
The University of Texas at Austin
Austin, Texas 78712
and
Daniel C. Barnes
Los Alamos National Laboratory
P. O. Box 1663
Los Alamos, New Mexico 87545

Abstract

The possibility of stabilizing the tilt mode in Field Reversed Configurations without resorting to explicit kinetic effects such as large ion orbits is investigated. Various pressure profiles, $P(\Psi)$, are chosen, including "hollow" profiles where current is strongly peaked near the separatrix. Numerical equilibria are used as input for an initial value simulation which uses an extended Magnetohydrodynamic (MHD) model that includes viscous and Hall terms. Tilt stability is found for specific hollow profiles when accompanied by high values of separatrix beta, β_{sep}. The stable profiles also have moderate to large elongation, racetrack separatrix shape, and lower values of $\bar{s}$, average ratio of Larmor radius to device radius. The stability is unaffected by changes in viscosity, but the neglect of the Hall term does cause stable results to become marginal or unstable. Implications for interpretation of recent experiments are discussed.

PACS: 52.65.+z; 52.55.Hc; 52.35.Py; 52.30.Bt

I. Introduction

The Field Reversed Configuration (FRC) is an example of a compact toroidal confinement concept.[1] The external field is that of a solenoid (perhaps with mirrors) but large diamagnetic currents reverse the magnetic field near the axis to form closed toroidal field lines. This configuration offers reactor advantages such as high β, coil geometry not linked with plasma torus, ease of plasma translation, no symmetry axis shielding, and an inherent separatrix that could serve as a natural divertor for high efficiency direct conversion of energy from fusion products.[2] A central question in FRC theory is stability with respect to the tilt mode, a global internal mode characterized by rotation of the plasma about an axis perpendicular to the symmetry axis. Ideal Magnetohydrodynamic (MHD) theory predicts instability: Intuitively, the plasma is a current dipole with its moment aligned anti-parallel to its external field. Quantitatively, for Hill's vortex solutions, the competition between stabilizing magnetic pressure and destabilizing current effects varies with elongation. For elongations higher than a critical value, stability is lost. Fluid theory predicts a growth time on the order of an axial Alfvén transit time,[3, 4, 5, 6]

$$\gamma_{\text{tilt}}^{0} = \frac{C\, V_{\text{Alfvén}}}{b} , \tag{1}$$

where $V_{\text{Alfvén}}$ is an average Alfvén velocity, C is a constant, on the order of unity and b is the separatrix half-length. External stabilization is difficult since perturbations are confined largely within the separatrix, as has been verified in fluid simulations.[1, 7] Nonlinear simulations see no saturation mechanism before total disruption.[8, 9] Subsequent single fluid theory has been unable to find stability for equilibria of experimental interest. While toroidal rotation can stabilize the mode,[5] the required rotation rate is much higher than observed in experiments. Effects from inclusion of the Hall term[10] and gyroviscous effects[11] indicate

that stability can be achieved for high elongations. With only a few recent exceptions,[12, 13] experiments do not observe tilt instabilities.[14, 15, 1] Recent analytic results indicate that the minimum stable elongation can be decreased by as much as 30% by varying the equilibrium separatrix shape, even for flat pressure profiles.[16] This together with improved analysis has led to the claim that most experimentally stable results can be explained. However, this analysis does predict that machines with a larger radius compared to the ion gyroradius will be tilt unstable.

More elaborate kinetic theoretical approaches show the possibility of stabilization by virtue of kinetic effects.[17] Many of the ion orbits in this regime are complex, resembling neither drifting Larmor orbits[18] nor betatron orbits.[19] Most experiments (with two recent exceptions[12, 20]) are of such a small size to allow large enough kinetic effects to increase the instability growth time to longer that the FRC lifetime.[17, 21, 19] A third exception is a cool FRC with high collisionality.[13] In that case the plasma may be so collisional ($\nu_{coll} > \Omega_{cyc}$) that fluid-like behavior is seen even in small devices.

FRC's with a large radius compared with the ion gyroradius would be more fluid-like and conventionally would be expected to be observably tilt unstable. Stabilization of the tilt mode by the presence of energetic beams may be possible. Estimates indicate that the required beam energy and total current are substantial but may not be unrealistic.[22, 23, 24] Preferential trapping of fusion products may provide a large amount of the required current.[25] Recently reported experimental results have been less clear. Tuszewski *et al.* have reported clear evidence of a tilt-like perturbation and a strong correlation of this tilt activity with degraded confinement.[12] This was explained as an effect of operating the device in a more fluid-like region of parameter space. Good agreement was found with probe signals predicted from fluid simulations and the actual observed signals. In some shots, however, the FRC partially survived the tilt event instead of completely dumping the contained density along open field lines. Preliminary results on the LSX experiment[20] have not seen correlation between tilt-

like signals [B_θ $n = 1$ axially even probe measurements] and confinement. Although LSX is expected to behave in an even more fluid-like manner.

It has recently been suggested that there may be another tilt mode stabilization mechanism — profile consistency.[26, 27] The fluid displacement in variational theory can be expressed in terms of first and second derivatives of the pressure profile $P(\Psi)$ where Ψ is the poloidal flux (plus other terms independent of $P(\Psi)$). The $P'(\Psi)$ term is always destabilizing while the $P''(\Psi)$ term can be either stabilizing or destabilizing depending on the sign of $P''(\Psi)$. Alternatively this is stated in terms of comparisons between a normalized current, $j/r = P'(\Psi)$, at the O-point and at the separatrix.

The purpose of this work is to investigate the tilt stability of equilibria with non-trivial pressure profiles. The basic question can be stated as: Do MHD or Hall fluid equilibria exist which are stable to tilt perturbations? Our numerical simulations indicate yes, for a class of special, but perhaps realizable equilibria. The approach is to search for a small set of fluid equilibria using standard elliptic equilibrium solvers and then to use these as the initial conditions for initial value fluid simulations. The subsequent analysis neglects explicit kinetic effects (but does include extensions to fluid theory such as viscosity and Hall terms). Since kinetic effects are generally considered stabilizing, this analysis may be viewed as a conservative estimate of stability in this regard. Additionally, this investigation may serve as an indicator of the possible effects of different equilibria upon stability. This especially includes modification of the FRC due to energetic ion components.[23, 24, 25]

The paper is organized as follows. Section II. describes the physical models and their numerical solution. Section III. describes the choice of pressure profile. Section IV. gives a set of equilibrium solutions and Sec. V. describes their dynamical behavior. Finally, Sec. VI. interprets these results and discusses their implications.

II. Hall Fluid Model and Numerical Formulation

FRC fluid theory has included various extensions to simple ideal MHD such as resistivity, equilibrium flow,[5, 10] nondiagonal pressure (ion gyro-viscosity[11]), and Hall terms[10] in their analysis. These extensions arise from the inclusion of physical effects which are neglected in ideal MHD. This work continues these practices for comparison with previous computational results. It also allows for precise identification of the effects upon stability of the model extensions, independently and in combinations. The plasma is modeled by the following dynamical equations:

$$\frac{\partial n}{\partial t} + \nabla \cdot (n\mathbf{u}) = 0 \,, \tag{2}$$

$$Mn\left[\frac{\partial \mathbf{u}}{\partial t} + \mathbf{u}\cdot\nabla\mathbf{u}\right] = \left(\frac{\mathbf{J}}{c}\times\mathbf{B}\right) - \nabla P - \nabla\cdot\vec{\Pi} \,, \tag{3}$$

$$\frac{\partial \mathbf{A}}{\partial t} = \mathbf{u}\times\mathbf{B} - \eta c^2\frac{\mathbf{J}}{c} - H\frac{c}{en}\left[\frac{\mathbf{J}}{c}\times\mathbf{B} - \nabla P_e\right] \,, \tag{4}$$

$$\frac{\partial S}{\partial t} + \nabla\cdot S\mathbf{u} = \frac{\gamma-1}{n^{\gamma-1}}\left[\eta\mathbf{J}^2 - \vec{\Pi} : \nabla\mathbf{u}\right] \,, \tag{5}$$

where n is the number density; $\mathbf{u}$, the flow velocity; M, the ion mass; $\mathbf{J}$, the current density; $\mathbf{B}$, the magnetic field; P, the total pressure; $\mathbf{A}$, the vector potential; η, the resistivity; S, an entropy density; P_e, the electron pressure; $\vec{\Pi}$, the viscous stress tensor; γ, the adiabatic constant; and H is an artificial variable used to include or exclude Hall effects. $H = 1$ utilizes the Hall terms while $H = 0$ ignores them. The derived quantities are defined by the following relations:

$$\mathbf{B} \equiv \nabla\times\mathbf{A} \,, \tag{6}$$

$$\frac{\mathbf{J}}{c} \equiv \left(\frac{1}{4\pi}\right)\nabla\times\mathbf{B} \,, \tag{7}$$

$$P = nT \,, \tag{8}$$

$$P_e = f_{te}P \,, \tag{9}$$

$$\bar{\bar{\Pi}} \equiv -(\nabla \mu \mathbf{u}) - (\nabla \mu \mathbf{u})^T + (\nabla \times \mu \mathbf{u}) \ , \tag{10}$$

$$S \equiv n^{\gamma-2} T \tag{11}$$

where f_{te} is a parameter determining the total pressure contained in electrons and μ is the viscosity coefficient.

The "Hall" term, $c/en\,[\mathbf{J}/c \times \mathbf{B} - \nabla P_e]$, results from the massless electron approximation to the generalized Ohm's law without the usual further assumption of wavelength small compared to spatial gradients.[28] Since FRC's have large β and the tilt mode is a global mode, effects from the Hall term may be of dynamical importance. Another way to understand the physical importance of the Hall term is from a two fluid formalism.[10] The massless electron approximation implies that the magnetic field is frozen to the motion of the electron fluid. In ideal MHD, further assumptions lead to the conclusion that $\mathbf{V}_e = \mathbf{V}_i$. Thus the Hall term measures the physical effects from different responses of ions and electrons to equilibrium and perturbed fields. The value of the artificial parameter H is selected at run-time for the simulation in order to include or exclude the Hall term effect.

We cast the equilibrium problem by taking the steady state limit of the dynamical equations with the extra assumptions of zero resistivity, zero viscosity, no Hall term, and no flow velocity. The geometry is specified as cylindrical (r, θ, z) coordinates with θ as the ignorable coordinate. We further assume zero toroidal field, B_θ, characteristic of FRC's . If we define the poloidal flux function as:

$$\Psi(r,z) \equiv \int_0^r B_z(r',z) r' \, dr' \ , \tag{12}$$

then the equilibrium equation,

$$\nabla P = \frac{\mathbf{J}}{c} \times \mathbf{B} \ , \tag{13}$$

reduces to the Grad-Shafranov relation:

$$\Delta^* \Psi \equiv r \frac{\partial}{\partial r} \frac{1}{r} \frac{\partial \Psi}{\partial r} + \frac{\partial}{\partial z} \frac{\partial \Psi}{\partial z} = -\frac{4\pi r^2}{c} \frac{dP}{d\Psi} \ . \tag{14}$$

It also implies that the pressure is entirely a function of the poloidal flux, $P = P(\Psi)$.

Experimental data to determine the functional dependence of P upon Ψ is not available. Most work has used either a rigid rotor profile, a linear profile, or an approximately linear profile. Recent transport calculations[27] indicate that either pressure profiles or resistivity profiles must be of a more complex structure in order to explain observed flux loss and particle loss. In this work, we examine profiles with more complex dependencies upon Ψ.

These models are investigated using numerical equilibrium and initial value codes. The equilibrium solver[29] iteratively solves Eq. (14) for $\Psi(r, z)$. Its domain is the region $0 < r < r_{\rm wall}$ and $0 < z < z_{\rm wall}$, assuming $\Psi(r, -z) = \Psi(r, z)$. Algorithmically, it is a descendant of previous 2-dimensional equilibrium studies.[30, 31, 7] The code set allows solution to both kinetic, rotating, or fluid plasmas. Only the fluid formulation is used in this investigation. The problem size was 45 cubic splines in the radial direction and 81 finite difference points in the positive z half-space.

The initial value simulation uses the FLX algorithm[32, 9] for 3-Dimensional spatial plus temporal plasma evolution. It numerically solves the dynamical model equations, Eqs. (2)–(5). The evolution is solved using a semi-implicit time advance. The dynamic fields are represented in r and z on a finite difference, staggered grid. The toroidal direction (θ) is mode expanded. This is the same numerical approach used to compare predicted and measured probe signals in recent experimental tilt observations.[12] Simulations examining beam effects on tilt stability also used an extension of this algorithm.[23, 24]

In these runs, 40 radial and 100 axial points were used. The axial points covered the region $-z_{\rm wall} < z < +z_{\rm wall}$, allowing for both even and odd axial dynamics. Since our goal is to study profile effects on tilt stability, only the modes with azimuthal index $n = 0$ and $n = 1$ are kept in these simulations. Nonlinear errors from neglecting higher mode couplings will not affect the conclusions about linear tilt stability.

The equilibria used in this investigation explore more fully different pressure (and hence

current) profiles. Specifically, here we examine equilibria where the functional dependence of $P(\Psi)$ on Ψ is different from piece-wise linear, or approximately piece-wise linear.

We will describe our equilibria in terms of conventional dimensionless FRC parameters. The first is a measure of the finite Larmor radius (FLR) corrections,

$$s \equiv \int_R^a \frac{rdr}{a\rho_i} , \tag{15}$$

where R is the radius of magnetic field null, a is the separatrix radius, and ρ_i is the local ion gyro-radius. A second measure is:

$$\bar{s} \equiv \frac{e}{c} \frac{|\Psi_0|}{\sqrt{MT(1-f_{te})}} \frac{1}{a} , \tag{16}$$

where $|\Psi_0|$ is the absolute value of the trapped flux. $\bar{s}$ is a quantity which can easily be calculated from numerically computed equilibria. Finally, S_* is defined by,[10]

$$S_* \equiv \sqrt{4\pi e^2 n_0 a^2/Mc^2} = \omega_{pi}\, a/c , \tag{17}$$

where n_0 is the plasma density maximum (density at O-point). The S_* is a measure of the importance of the Hall term in the plasma dynamics.

The relations among s, $\bar{s}$, and S_* can be derived by considering the case of highly elongated FRC equilibria where midplane field line curvature can be neglected. Pressure balance relates the peak pressure at the O-point to the external magnetic field, $P_0 = n_0 T_0 = B_{ext}^2/8\pi$. Thus in such high beta systems, the plasma and cyclotron frequencies are not independent, but are related by,

$$\omega_{pi} = \frac{c}{\sqrt{2}\, v_{ti}} \omega_{ci}^{ext} = \frac{c}{\sqrt{2}} \rho_i^{ext} , \tag{18}$$

where it is understood that the density at the O-point is used in the calculation of ω_{pi} and the external field is used in ω_{ci} and ρ_i.

We can relate s and S_* as:

$$S_* = \frac{\sqrt{2}}{\lambda} s , \tag{19}$$

where

$$\lambda \equiv \rho_i^{ext} \left\langle \frac{1}{\rho_i} \right\rangle \tag{20}$$

and

$$\langle A \rangle \equiv \frac{\int_R^{r_{sep}} A r\, dr}{\int_R^{r_{sep}} r\, dr} , \tag{21}$$

with the additional note that $R = r_{sep}/\sqrt{2}$. Note that $0 < \lambda < 1$; λ will be small for small internal magnetic fields. We can also relate s and $\bar{s}$ through

$$\bar{s} = \frac{s}{\sqrt{1 - f_{te}}} , \tag{22}$$

when it is noted that Eq. (12) implies $\int_R^{r_{sep}} Br\, dr = \Psi_0$. Thus, $\bar{s}$ incorporates into s the partial cancellation of the Hall term effect arising from the ∇P_e term.

On the one hand, S_* is a measure of how the electron and ion fluids responses differ while s measures the importance of FLR and/or finite ω/ω_{ci} effects. For small FLR, the ion and electron response are identical. Therefore it is reasonable for s and S_* to scale similarly. The Hall term effect and other non-ideal MHD effects will be most pronounced for low s (and hence S_*). Practically, $\bar{s}$ is a better measure of these effects since it takes into account the details of whether the internal field is depressed (i.e. the factor of λ). The question of a depressed internal field is important since it is one of the principle features of hollow equilibria.

III. Profile Choice

In addition to the choice of physical model, the unique equilibrium solution depends on the specification of additional parameters. The boundary choice is a perfect conducting flux conserver at a fixed radius $r = r_w$ and a free boundary at $z = \pm z_w$. The flux at the wall is fixed as Ψ_w. The functional relationship $P(\Psi)$ must also be specified. Since the Grad-Shafranov equation is in general nonlinear, additional parameters may be necessary

to uniquely specify the solution.[30, 31] The growth rate of the tilt perturbations, γ_{tilt}, may depend upon a multitude of parameters.

These may include geometrical factors (such as separatrix radius a; $X_s \equiv a/R_w$; separatrix length, b; separatrix elongation, $E \equiv b/a$), physical quantities (such as total trapped flux Ψ_0; midplane averaged beta, $\langle\beta\rangle$; temperature profile; pressure profile), experimental parameters (such as bias field; fill pressure; formation method; etc.), or model determining parameters (such as s; velocity; and transport coefficients),

$$\gamma_{tilt} = \gamma_{tilt}(\Psi_w, \Psi_0, r_w, z_w, a, b, E, X_s, P(\Psi), \langle\beta\rangle, B_{bias}, P_{fill}, s, \eta, \mu, \ldots) . \qquad (23)$$

Many of these quantities are not independent. The elongation is just the ratio of separatrix length to separatrix width. The quantity $\langle\beta\rangle$ depends strongly on P_{fill}; $\langle\beta\rangle$ is given in terms of X_s from axial force balance.[1] Experimental evidence relates $P(\Psi)$, η, and X_s.[27] Only small portions of parameter space may be tractably examined at once. An ansatz must be invoked to limit the parameters to survey. In this work we investigate possible profile functions. Specifying $P(\Psi)$ will almost uniquely specify the equilibrium. Since the equilibrium problem is nonlinear (for a general $P(\Psi)$ profile), there may be more than one solution. In addition if the length of the separatrix, b, is specified, then in practice the equilibrium is uniquely specified.[30, 31] Other parameters that determine γ_{tilt} that have not been explicitly specified are thus implicitly determined from the above conditions. The choice of $P(\Psi)$ serves to specify most of these implicit relationships. Equilibrium characteristics such a racetrack or elliptic separatrix shape and elongation will fall out from the profile choice as opposed to being specified parametrically.

Most previous theory has assumed that $P(\Psi)$ was linear in Ψ while exploring other (mostly geometric) effects of varying other parameters.[4, 1] There is an analytic solution with a nonlinear $P(\Psi)$ which has been used in some FRC tilt studies.[6, 33] However, this particular profile has a $P(\Psi)$ form that does not allow independent specification of $P'(\Psi)$ and $P''(\Psi)$. It

is not clear whether such a restriction can allow enough flexibility to explore the competing effects from the $P'(\Psi)$ and $P''(\Psi)$ terms. To our best knowledge, all known numerical studies (except one[34]) on FRC tilt stability assumed pressure profiles that were linear, piecewise linear, or an approximation thereof.[7, 30] Even though these equilibrium solvers have the ability to find numerical solutions for nonlinear pressure profiles, stability studies have not looked at such profiles. A separate numerical approach[35, 36] to numerical equilibria chooses the entropy function instead of a $P(\Psi)$ profile. The implied $P(\Psi)$ profile is not linear, but again, it does not appear to have been used in stability studies.

The one exception is an early numerical simulation.[34] The current profile chosen in that study varied sinusoidally with a polynomial of the flux. The profile concentrated normalized current, j_θ/r, of the same magnitude at both the separatrix and the O-point. Depending on the choice of a profile index, the normalized current between the O-point and separatrix and between the O-point and axis was higher or lower. That study did not report any large scale instability consistent with tilting for tens of Alfvén transit times.

Our choice of pressure profile is designed to investigate the possibility of hollow profiles having a stabilizing effect.[26, 27] We allow the pressure profile to be a nonlinear function of the flux function. This may perhaps be regarded as an allowance for the possibility of a self-organizing tendency of FRC plasmas.[37, 26] We choose a parameterized profile that allows the concentration of current at either the O-point or near the separatrix:

$$P(\Psi) = P_0\mu(\chi) = \begin{cases} P_0(K_0 - \chi - \frac{1}{2}D\chi^2) & \chi \leq 0 \\ P_0\left(\frac{1}{F}e^{-F\chi}\right) & \chi \geq 0\,, \end{cases} \tag{24}$$

where P_0 is a normalizing constant for the pressure. Varying P_0 during the iterative solution process will serve to fix the separatrix length. $\mu(\chi)$ is the profile shape function. χ is the normalized poloidal flux, $\chi \equiv \frac{\Psi}{|\Psi_0|}$, and $\Psi_0 < 0$ is the trapped flux, the flux at the O-point. K_0, D, and F are profile parameters. They are specified by four conditions: continuity of $\mu(0)$ and $\mu'(0)$ at the separatrix; $\beta_{sep} \equiv \frac{P(\Psi=0)}{P(\Psi_0)}$ given; and D given. Solving for F and K_0,

one obtains,

$$K_0 = \frac{\beta_{sep}(1 - D/2)}{1 - \beta_{sep}} , \tag{25}$$

$$F = \frac{1}{K_0} . \tag{26}$$

Hollowness and peakedness of the profile are defined as parameters that describe the current (or equivalently pressure) distribution within the separatrix.[27] Hollowness or peakedness are defined by comparing local values of $P'(\Psi) = j_\theta / r$. A "peaked" profile has its current concentrated at or near the O-point. Conversely, a "hollow" profile has the current concentrated near the separatrix (away from the O-point). In terms of the pressure profile, a peaked profile will be very peaked around the O-point and fall rapidly, even for regions still inside the separatrix. A hollow pressure profile will remain large and flat until very near the separatrix where it will then decrease. A flat profile has $P(\Psi)$ linear in Ψ inside of the separatrix. This corresponds to a current density which depends linearly on radius. In this case $P''(\Psi) = 0$. It should be noted that the discussion of "hollowness," "peakedness," and "flatness" are defined in terms of the variation of P with Ψ. Reconstruction of the spatial dependence of P will require further knowledge about the spatial solution for Ψ.

For this profile choice, the parameter D specifies the hollow or peaked equilibrium character. $D = 0$ gives a flat profile; $D > 0$, hollow; and $D < 0$ peaked. It should be noted that D is not identical to h, a previously defined hollowness parameter,[27] however, the qualitative notions of "hollowness" and "peakedness" are the same. This choice of profile function gives $P''(\Psi) \propto -D$ inside the separatrix. Thus D is a control parameter to increase or decrease the relative importance of the effect of the $P''(\Psi)$ term. The destabilizing $P'(\Psi)$ term is also modified by D: $P'(\Psi) \propto -1 - D\chi$. Since $-1 < \chi < 0$, D acts to decrease the tilt mode driven by $P'(\Psi)$ for $0 < D < 1$. On the exterior flux surfaces, $P''(\Psi) > 0$. This does not cause instability since the field lines have good curvature in this region.

This profile possesses adequate generality to probe possible profile stabilization effects

while only requiring exploration of a small 2-dimensional parameter space. All equilibrium parameters are specified by the choices of boundary conditions, model formulation, profile functional form, imposed separatrix length, and by the point chosen in the (β_{sep}, D) parameter space.

IV. Equilibrium Solutions

Here we report a series of equilibrium solutions. They are broken into two sets, $\beta_{sep} = 0.1$ and $\beta_{sep} = 0.6$. These two sets are then scanned in D from peaked to flat to hollow values of D. The dimensional characteristics of these equilibria approximately correspond to previous numerical simulations.[23, 9] The dimensionless characteristics of some of these profiles are summarized in Table I. As can be seen, varying β_{sep} and D with this profile choice also entailed changes in other physically meaningful variables. In this sense, what was varied and what was fixed is not a division of parameter space into an orthogonal set of physically meaningful quantities. Contour plots of Ψ for some of these equilibria are shown in Fig. 1. Several features are observed for this parameter scan. Ratio of plasma radius to wall radius, X_s is smaller for higher β_{sep} and for more hollow profiles.

The separatrix half-length b is a fixed input parameter. Therefore the elongation varies proportionally to X_s. However, a local pseudo-elongation can be defined in terms of the length versus the width of internal flux surfaces. This may be more physically meaningful since the actual $\Psi = 0$ contour, being a separatrix, is susceptible to small perturbations. This is especially pronounced for peaked profiles. This local pseudo-elongation may also be viewed as a closer approximation to the local field line curvature. In the literature, this is often referred to as the question of a racetrack vs. elliptical shaped flux surface.[7] Elliptical profiles tend to have a constant normalized curvature, while racetrack equilibria have almost all of their curvature concentrated into a small endcap near $z = b$. Peaked profiles ($D < 0$) lead to elliptical, low pseudo-elongation profiles, while hollow ($D > 0$)

profiles cause racetrack, or high pseudo-elongation profiles.

The volume averaged β, $\langle\beta\rangle_{\rm vol}$, is larger for the $\beta_{\rm sep} = 0.6$ equilibria (note that volume averaged β, $\langle\beta\rangle_{\rm vol}$, is different from midplane averaged β used in the relation $\langle\beta\rangle_{\rm mid} = 1 - X_s^2/2$). For fixed $\beta_{\rm sep}$, $\langle\beta\rangle_{\rm vol}$ increases for hollow profiles, as expected. Also note that for the given profile choice, high $\beta_{\rm sep}$ and hollow profiles tend toward decreased plasma volume, peak plasma pressure and actual trapped flux (Ψ_0). Low Ψ_0 can be partially explained in terms of the boundary condition fixing Ψ_w. A smaller X_s implies a smaller external field, which is one of the natural normalization parameters of the equilibrium. However, for Ψ_0 there is an additional effect. Two equilibria with identical X_s will have differing values of Ψ_0 depending on their degree of hollowness.

The trapped flux Ψ_0 is usually not directly measured in experiments, but rather is inferred from the measured excluded flux radius and an assumption about the $P(\Psi)$ profile.[15, 1] Experiments would report identical inferred values for Ψ_0, while their actual values may vary. Direct experimental observation of hollowness of profile (and hence also Ψ_0) requires direct knowledge of P as a function of radius, $P(r)$. It is necessary to perform interferometry at many different radii in order to differentiate hollow, flat, and peaked profiles experimentally, since this distinction relies on the second derivative of the pressure. Figure 2 shows normalized current, $\frac{|j_\theta(r)|}{rB_{\rm wall}}$, and pressure profiles $P(r)$ at the midplane for some of the $\beta_{\rm sep} = 0.6$ equilibria. While the distribution of current density varies greatly as D is varied from highly peaked to highly hollow, the pressure profile is only mildly modified. It is not clear that previous experiments could have distinguished hollow and peaked profiles from previous interferometry data that had only modest numbers of radial data points and shot to shot variation.[1, 38]

V. Dynamical Simulation Results

These equilibrium solutions were then used to initialize the dynamical simulation. An initial perturbation velocity of peak amplitude equal to 1% of $V_{\text{Alfvén}}$ was added. The functional form of this perturbation resembles other compressionless, internal trial functions.[4, 7, 23] The objective was to determine γ_{tilt} for each equilibrium and compare it to γ^0_{tilt}. The simulation parameters were nominally similar to the FRX-C/LSM experiment.[39] They ran for 25 μ sec, which is about 5 growth periods. The *a priori* hypothesis was that γ_{tilt} would be considered independent of pressure profile in this parameter search if the normalized growth rate, $\hat{\gamma} \equiv \gamma_{\text{tilt}}/\gamma^0_{\text{tilt}}$, is within a factor 2 of unity. Geometric manipulation of the equilibrium separatrix shape for flat profiles can change the growth rate by as much as a factor of 2.[4, 40, 7] Any profile modification effect is required to lie outside of this noise range. The γ_{tilt} was measured from fits to the kinetic energy in the $n = 1$ mode.

The measured growth rates are summarized in Table I. Figure 3 shows the time histories of $n = 1$ kinetic energy. For the $\beta_{\text{sep}} = 0.1$ cases the saturation amplitude decreased as the profile changed from peaked to hollow but the growth rate (as measured by the slope on the logarithmic plot) is essentially unchanged. Separate diagnostics show that all magnetic field lines are open after the peak amplitude in all cases. This allows parallel motion from inside the separatrix to the end walls. Separate diagnostics also show a depletion of the central pressure peak on an Alfvén transit time scale. Similar traces are shown for the $\beta_{\text{sep}} = 0.6$ cases. Again the peak tilt amplitude was lower and the time of tilt peak was longer for the more hollow cases, but the effect was more pronounced. The scale for the $\beta_{\text{sep}} = 0.1$ case is about 60 times larger than the scale for the $\beta_{\text{sep}} = 0.6$ case. A more surprising feature emerges in the logarithmic traces, where the actual growth rates (determined from the slope of the traces) show a decreasing trend with increasing hollowness. Figure 4 plots $\hat{\gamma}_{\text{tilt}}$ as a function of hollowness. The hollow, high β_{sep} profiles show a clear trend toward lower growth

rates. These features are reinforced when traces of field lines are examined.

Figure 5 shows a sample of integrated magnetic field lines. The field lines open up not only for the flat profile cases (Figs. 5a and 5c) but also for the $\beta_{sep} = 0.1$ hollow cases (Fig. 5b). However, the $\beta_{sep} = 0.6$ $D = 0.8$ and $\beta_{sep} = 0.6$ $D = 0.85$ cases (Figs. 5d-5g) maintain closed field lines for up to 50 μ sec, further indicating tilt stability. 50 μ sec is about 10 growth times and is a significant fraction of τ_ψ, the flux confinement time. At this late time, the configuration has changed considerably owing to simple transport effects.

Finally, Fig. 6 shows the perturbation mode structure well into the simulation for selected profiles. These are snapshots of the $n = 1$ poloidal components of the velocity after development of the natural mode structure from the initial perturbation and noise. The flat profile cases (Figs. 6a and 6c) show the usual tilt mode displacement as an almost rigid rotation perpendicular to the symmetry axis. The hollow profiles (Figs. 6b, 6d, and 6e) show a mode structure much more localized to the end regions as previously observed [7] This is explained by the concentration of instability inducing field line curvature in the end regions. However, the $\beta_{sep} = 0.1$, $D = 0.8$ case (Fig. 6b) shows an interesting new feature. The instantaneous velocity streamlines are localized into 3 cells of length $2b/3$ instead of the normal single cell of size $2b$ as would be the case for rigid tilting. Similar effects have previously been noted in Hall fluid simulations.[9] At later times, this mode structure evolves decreasing the central cell and enlarging the outer cells until they all finally merge late in the simulation into a normal tilt type mode structure. The $\beta_{sep} = 0.6$, $D = 0.8$ and $\beta_{sep} = 0.6$, $D = 0.85$ cases (Figs. 6d and 6e) had less well defined mode structures. The mode was very localized to the endcaps with no other discernible structure.

Next we consider whether the apparent tilt stability of the hollow high β_{sep} profiles is robust to minor numerical or physical modifications of parameters. Is the behavior due to coarseness of numerical grid? Is the behavior due to a short simulation time? Is the behavior due to viscous effects? Is the behavior due to the Hall term? Five additional dynamical

simulations were conducted to address these questions. They extended the simulation to 50 μsec (approximately 10 growth times). Two of the cases were repetitions of the $\beta_{sep} = 0.6$, $D = 0.8$ and $\beta_{sep} = 0.6$, $D = 0.85$ runs above. They served as the baseline cases to measure the effect of these model and algorithmic variations. The purpose is to determine whether questions about simulation integrity and physical model can cause a simulation to vary more than the variation caused by changing the D parameter from a value of 0.80 to 0.85. The other three simulations were repetitions of the $\beta_{sep} = 0.6$, $D = 0.85$ case with modifications. One modification was to run the simulation with a grid doubled in both the r and z directions. Another was to halve the viscosity coefficient, and the final case was run with the Hall term absent ($H = 0$ in Eq. (4)). The time history of the $n = 1$ mode kinetic energy is shown in Fig. 7. The vertical scales on the linear plots are about a factor of 1000 smaller than for the $\beta_{sep} = 0.1$ cases in Fig. 3, and a factor of 20 smaller than the $\beta_{sep} = 0.6$ cases in Fig. 3. The effect of doubling the grid or halving the viscosity was less than the effect of changing D from 0.85 to 0.80.

The effect of neglecting the Hall term changed the trace significantly. Moreover, separate diagnostics showed that this $H = 0$ case could not be classified as absolutely tilt stable, if for no other reason than that the field lines were opening up by the end of the simulation as shown in Fig. 8. However, the level of tilt activity for the $H = 0$ case was still much less than either the hollow $\beta_{sep} = 0.1$ or the flat profile cases.

Nevertheless, Fig. 7 shows that except for the $H = 0$ case, the level of $n = 1$ kinetic energy differs little from its initial perturbation value and is characterized by slow evolution or oscillation rather than exponential growth. The $H = 0$ case can be seen as a long 40 μsec oscillation or an unstable mode with a saturation 2 to 3 e-foldings from onset. The initial value numerical simulation technique can never reliably determine between these possibilities.

The effect of the Hall term appears important to tilt stability. A final series of runs was conducted to focus on this issue. Simulations were conducted in pairs for various values of D

(with $\beta_{sep} = 0.6$). One member of the pair included the Hall term while the other neglected it. The results are shown in Fig. 9. In all instances, the kinetic energy in the $n = 1$ tilt mode is less when the Hall term is included. For the flat profile case, the two traces are almost identical. For the hollow profiles (large values of D) the traces diverge. Beyond a value for D of about 0.5, increasing hollowness does not decrease tilt activity if the Hall term is neglected. The $D = 0.85$ run without the Hall term more closely resembles a value of $D = 0.50$ than $D = 0.85$ when cor.pared with runs that included the Hall effect.

VI. Discussion and Implications

We set out to investigate profile effects upon tilt stability. The conjecture that hollow profiles will have a tendency toward reduced tilt activity is borne out by simulation. However, hollowness alone is not sufficient to eliminate unstable growth. We have found that the effect is only sufficient for high values of β_{sep}. It should be noted that an initial value simulation cannot give reliable information on contours of marginal stability. Typically at marginal stability the growth rates approaches zero and the modes become oscillatory. A half period of oscillation is difficult to distinguish from growth and saturation when kinetic energy histories are the only diagnostic. Future numerical variational modeling and variational theory may give more concrete statements about marginal stability contours.

Further, if the Hall effect is neglected, there appears to be a lower bound on the effectiveness of hollowness. Equilibrium profiles with hollowness parameters below this bound experience "diminishing returns" with respect to the ability of additional hollowness to suppress instability. Moreover, the values of hollowness required to achieve stability are below this bound. Increasing the hollowness of an equilibrium reduces the strength, and to some point the growth rate of the tilt instability. However, only when we combine hollowness with high β_{sep} and the inclusion of the Hall effect do we see simulations that appear stable. It should be noted that these relationships were observed for only a particular class of equilib-

ria. These results may not generalize to different equilibria with differing sets of fixed and varying equilibrium parameters.

In these simulations we chose $f_{te} = 0$. This cold electron assumption is in accord with previous kinetic calculations[17] and is a fair approximation of low fill pressure experimental conditions soon after formation.[41, 39] The Hall term is proportional to

$$\frac{\mathbf{J}}{c} \times \mathbf{B} - \nabla P_e = \frac{\mathbf{J}}{c} \times \mathbf{B} - \nabla P + (1 - f_{te})\nabla P = (1 - f_{te})\nabla P \ , \tag{27}$$

when one makes use of the non-rotating equilibrium condition, Eq. (13). Thus the effect of errors in choice of f_{te} in non-rotating equilibria is equivalent to varying the ad hoc Hall Parameter H. The physical value is $H = 1$. Using a value of f_{te} less than its physical value thus overestimates the effect of the Hall term, but by no more than a factor of 2. Additionally, the simulation run with $H = 0$ has no dependence on the choice of f_{te}. Since even this run showed marked departure from usual tilt behavior, we conclude that there is a significant reduction in tilt activity independent of the Hall term for hollow profiles. The inclusion of the Hall term leads us to further conclude that we have reached a point in (β_{sep}, D) parameter space of tilt stability.

That hollow profiles with high β_{sep} can stabilize the tilt mode is at first surprising. This is emphasized when it is realized that this simulation neglected many aspects of physical FRC behavior that might act as a stabilization mechanism such as large orbit ions.[19] It is known that kinetic stabilization for small s is possible,[17] By neglecting kinetic effects, these simulations appear to apply to the $s \rightarrow \infty$ limit. However, selected kinetic effects are explicitly re-introduced in the form of viscosity and Hall terms. The question then becomes one of whether the observed stability is ascribable to previous extensions of MHD theory. Variational theory has indicated that if the parameter, $S_* \equiv a\omega_{pi}/c$, is small enough, large elongations may be stabilized. Stability is found for $S_* < C\,E$, where C is a model depend factor of order unity and E is the plasma elongation. For Hall fluids, $C_{hall} \approx 1$.[10]

For gyroviscous theory $C_{gyro} \approx 1.6$.[11] However, S_* is not a good figure of merit for assessing hollow profile effects. Two equilibria that have identical external fields, but differing levels of hollowness in their pressure profiles will nevertheless have the same value for S_*, even though $\bar{s}$ may differ radically for the equilibria, since hollowness can drastically alter the value of $|\Psi_0|$. Thus $\bar{s}$ is more appropriate for characterizing equilibria, when pressure profiles have different hollowness values. Equivalently, it can be stated that $\bar{s}$ is preferable to S_* since it considers the effect of midplane averaging in the factor of λ. Table I lists values of $\bar{s}$ for these runs and Fig. 10 graphs $\hat{\gamma}$ versus $\bar{s}$. The trend to stability correlates well with $\bar{s}$. We draw the conclusion that the effect of hollow profiles is to provide additional stabilization apart from previously considered effects. The fact that the exclusion of the Hall term causes the stable cases to become marginal or even unstable supports this notion.

The addition of hollowness to this analysis may come in many forms. First, the proportionality constant C may depend on the value of a hollowness parameter. Second, the left side of the relation may be S_*^{eff}, an effective S_* that is corrected for the low internal magnetic field. However, the relationship may be a more complex synergistic relation with various threshold requirements. This study is unable to distinguish between these possibilities. Comparison of analytic results with computational results is difficult for two additional reasons. First, analytic equilibria and simulation equilibria differ. Second, an initial value simulation will naturally pick the most unstable mode while variational calculations often have limited trial functions. Previous simulation[9] has indicated that for small values of S_* a new, more complex unstable mode emerges. They found that the instability growth rate could not be reduced below about 50% of γ_{tilt}. Such resistance to further reduction in γ may indicate that a new mode is dominating the dynamics. Such may be the case for the hollow, no Hall, simulations presented here.

Experimental comparisons require close examination of equilibrium conditions in order to determine whether comparisons of nominally similar shots are actually comparable. Di-

agnosis, let alone control, of parameters such as β_{sep} and hollowness is not evident for many experiments. It may depend on details of formation and device specificity. This may explain discrepancies regarding effects of tilt perturbations in current generation, larger s experiments.[12, 20]

While this work suggests that the effect of hollowness is to improve the marginally stable s/E ratio toward shorter elongations and higher s, it cannot be ruled out that its effect on tilt stability may be more complex. This effect is important in FRC reactor analyses.[2] A stable path from formation through compression and heating until ignition must be maintained quasi-statically at all times. During these stages both s and E can vary by factors as much as 3 to 5. Additional stabilization due to hollowness can relax reactor design criteria, allowing easier or more confident paths to ignition.

The implication for beam stabilization is also worth noting. Traditionally, it has been considered that FRC's with large values of s could be stabilized using energetic ions.[23, 2] Profile stabilization is most effective for moderate to long elongations (as are previous Hall fluid and gyroviscous results). Beam stabilization depends on a resonant condition between the axis encircling frequency and the axial betatron oscillation.[22] Tuning to this resonance requires an increase in betatron frequency by decreasing elongation. When the equilibrium is not tuned to resonance, the critical beam current needed for stabilization increases. Thus profile stabilization and beam stabilization are more effective for different equilibrium characteristics. Whether these conditions are compatible or exclusive must be addressed. That is, do equilibria exist where both effects are strong enough to insure stability or must equilibria be designed for either extremely large or small elongations to take advantage of only one effect in isolation?

Finally, these results for profile stabilization may have consequences in transport analyses. It is often assumed that as experimental devices became larger that β_{sep} would naturally decrease to almost negligible levels. Larger experiments have not observed this trend in β_{sep}.

These simulations found the possibility for stability only when hollowness was coupled to high β_{sep}. High β_{sep} may be an inherent co-requisite for stability, or high β_{sep} may simply serve to decrease the $\bar{s}$ of the equilibrium. High β_{sep} implies a need for some form of plasma confinement on the open field lines beyond the separatrix. Moreover, the necessity of maintaining high β_{sep} may dominate the determination of global FRC confinement characteristics. This will necessitate consideration of plasma in the region just beyond the separatrix. It should be noted that hollow current profiles may not be constant on resistive time scales. Current at the field null is small as is the total trapped flux. Therefore hollow profile effects upon τ_ψ, the flux lifetime, are not clear. Yet the large currents near the separatrix in hollow profiles point to decreased particle confinement time, τ_n, and resistive evolution towards flatter profiles.

Acknowledgments

One of the authors (JWC) would like to acknowledge valuable conversations with L. C. Steinhauer, M. Tuszewski, R. L. Webster, and D. J. Rej. The computations were performed on the National Energy Research supercomputers (NERSC). This work was support by the U. S. Department of Energy contract #DE-FG05-80ET-53088.

References

[1]M. Tuszewski, Nucl. Fusion **28**, 2033 (1988).

[2]W. Kernbichler, M. Heindler, H. Momota, Y. Tomita, A. Ishida, S. Ohi, M. Ohnishi, K. Sato, G. H. Miley, H. L. Berk, W. Dove, M.-Y. Hsiao, R. Lovelace, E. Morse, J. Santarius, L. C. Steinhauer, M. Tuszewski, and D. Barnes, In Plasma Physics and Controlled Nuclear Fusion (International Atomic Energy Agency, Vienna 1991), Vol. 3, p. 555.

[3]M. N. Rosenbluth and M. N. Bussac, Nucl. Fusion **19**, 489 (1979).

[4]R. A. Clemente and J. L. Milovich, Physics Letters **85A**, 148 (1981).

[5]R. A. Clemente and J. L. Milovich, Phys. Fluids **26**, 1874 (1983).

[6]R. A. Clemente and C. E. Grillo, Phys. Fluids **27**, 658 (1984).

[7]J. L. Schwarzmeier, D. C. Barnes, D. W. Hewett, C. E. Seyler, A. I. Shestakov, and R. L. Spencer, Phys. Fluids **26**, 1295 (1983).

[8]F. Brunel and T. Tajima, Phys. Fluids **26**, 535 (1983).

[9]R. D. Milroy, D. C. Barnes, R. C. Bishop, and R. B. Webster, Phys. Fluids B **1**, 1225 (1989).

[10]A. Ishida, Phys. Fluids **31**, 3024 (1988).

[11]L. C. Steinhauer and A. Ishida, Phys. Fluids B **2**, 2422 (1990).

[12]M. Tuszewski, D. C. Barnes, R. E. Chrien, J. W. Cobb, D. J. Rej, R. E. Siemon, and D. P. Taggart, Phys. Rev. Lett. **66**, 711 (1991).

[13]W. F. Pierce, R. J. Maqueda, R. Farengo, and R. D. Brooks, In Bull. Am. Phys. Soc. **36**, 2461 (191).

[14]W. T. Armstrong, R. K. Linford, J. Lipson, D. A. Platts, and E. G. Sherwood, Phys. Fluids **24**, 2068. (1981).

[15]R. E. Siemon, W. T. Armstrong, D. C. Barnes, R. R. Bartsch, R. E. Chrien, J. C. Cochrane, W. N. Hugrass, Jr. R. W. Kewish, P. L. Klinger, H. R. Lewis, R. K. Linford, K. F. McKenna, R. D. Milroy, D. J. Rej, J. L. Schwarzmeier, C. E. Seyler, E. G. Sherwood, R. L. Spencer, and M. Tuszewski, Fusion Technology **9**, 13 (1986).

[16]A. Ishida, R. Kanno, and L. C Steinhauer, Phys. Fluids B **4**, 1280 (1992).

[17]D. C. Barnes, J. L. Schwarzmeier, R. Lewis, and C. E. Seyler, **Phys. Fluids 29**, 2616 (1986).

[18]C. E. Seyler, J. F. Krall, L. Sparks, and R. N. Sudan, Nucl. **Fusion 24, 1013 (1984).**

[19]R. Horiuchi and T. Sato, Phys. Fluids B **2**, 2652 (1990).

[20]J. T. Slough, A. L. Hoffman, R. D. Milroy, and E. A. Crawford, **Phys. Rev. Lett. 69, 2212** (1992).

[21]E. J. Horowitz, Ph.D. Dissertation, University of Califronia, Davis (Lawrence Livermore National Laboratory), 1987.

[22]Y. Nomura, J. Phys. Soc. Japan **54**, 1369 (1985).

[23]D. C. Barnes and R. D. Milroy, Phys. Fluids B **3**, 2609 (1991).

[24]J. W. Cobb, T. T. Tajima, and D. C. Barnes, In Bull. Am. Phys. Soc. **35**, 2115 (1990).

[25]H. L. Berk, H. Momota, and T. T. Tajima, Phys. Fluids **30**, 3548 (1987).

[26]L. C. Steinhauer, E. A. Crawford, R. D. Milroy, and J. T. Slough, In Bull. Am. Phys. Soc. **35**, 2114 (1990).

[27]L. C. Steinhauer and A. Ishida, Phys. Fluids B **4**, 645 (1992).

[28]N. A. Krall and A. W. Trivelpiece, *Principles of Plasma Physics*, (San Fransisco Press, Inc., San Fransisco, 1986), pp. 88-95.

[29]R. B. Webster, J. L. Schwarzmeier, H. R. Lewis, C.K. Choi, and W. K. Terry, Phys. Fluids B **3**, 1026 (1991).

[30]R. L. Spencer and D. W. Hewett, Phys. Fluids **25**, 1365 (1982).

[31]D. W. Hewett and R. L. Spencer, Phys. Fluids **26**, 1299 (1983).

[32]D. C. Barnes, R. C. Bishop, R. D. Milroy, and D. D. Schnack, **"Flexible, Semi-Implicit** Alogirthms for Bounded Multi-Dimensional MHD Calculations" **to appear in J. Comput.** Phys.

[33]R. Farengo, Phys. Fluids B **4**, 280 (1992).

[34]D. C. Barnes and D. V. Anderson, Phys. Rev. Lett. **46**, 1337 (1981).

[35]D. E. Shumaker, J. Comput. Phys. **53**, 456 (1984).

[36]D. E. Shumaker, Fusion Technology **9**, 75 (1984).

[37]V. I. Petviashvili and V. V. Yan'kov, In *Reviews of Plasma Physcis*, edited by B. B. Kadomtsev (Consultants Bureau, New York, 1989), Vol.14 p.1.

[38]R. E. Chrien and S. Okada, Phys. Fluids **30**, 3574 (1987).

[39]D. J. Rej, M. Tuszewski, D. C. Barnes, A. D. Bailey, G. A. Barnes, M. H. Baron, R. E. Chrien, J. W. Cobb, A. Ishida, R. E. Siemon, J. L. Staudenmeier, S. Sugimoto, D. P. Taggart, T. Takahashi, R. B. Webster, and B. L. Wright, In Plasma Physics and Controlled Nuclear Fusion (International Atomic Energy Agency, Vienna 1991), Vol. 2, p. 647.

[40]J. H. Hammer, Nucl. Fusion **21**, 488 (1981).

[41]D. J. Rej and W. T. Armstrong, Nucl. Fusion **24**, 177 (1984).

β_s	D	$\hat{\gamma}$	$\sigma_{\hat{\gamma}}$	h	X_S	$\langle\beta\rangle_{vol}$	E	$\Psi_{0\ (mWb)}$	$\bar{s}$
0.1	-1.00	1.41	0.17	1.21	0.83	0.43	2.80	9.05	12.49
0.1	-0.50	1.28	0.17	1.13	0.81	0.48	2.88	7.55	10.69
0.1	0.00	1.26	0.17	1.00	0.77	0.56	3.01	5.58	8.26
0.1	0.50	1.32	0.17	0.76	0.69	0.67	3.34	3.12	5.12
0.1	0.75	1.32	0.26	0.53	0.63	0.74	3.70	1.83	3.33
0.1	0.80	1.29	0.26	0.46	0.59	0.77	3.91	1.48	2.85
0.6	-1.00	1.44	0.13	1.21	0.53	0.72	4.99	1.20	2.60
0.6	-0.50	1.18	0.11	1.13	0.51	0.73	4.86	1.05	2.33
0.6	0.00	0.83	0.07	1.00	0.50	0.77	4.74	0.91	2.07
0.6	0.50	0.18	0.17	0.75	0.46	0.83	5.00	0.63	1.54
0.6	0.75	0.07	0.26	0.53	0.41	0.88	5.63	0.40	1.09
0.6	0.80	0.01	0.26	0.46	0.39	0.89	5.88	0.33	0.97
0.6	0.85	-0.04	0.26	0.38	0.38	0.90	6.16	0.28	0.85

Table I Characteristics of equilibrium solutions, including: Separatrix Beta, β_{sep}; Hollowness Parameter, D; Normalized Growth Rate, $\hat{\gamma}$; Normalized Growth Rate Error, $\sigma_{\hat{\gamma}}$; Hollowness Parameter, h; Ratio of Separatrix to Wall Radius, X_S; Volume Averaged Beta, $\langle\beta\rangle_{vol}$; Elongation, E; Trapped Flux, Ψ_0; Kinetic Effect Parameter, $\bar{s}$

List of Figures

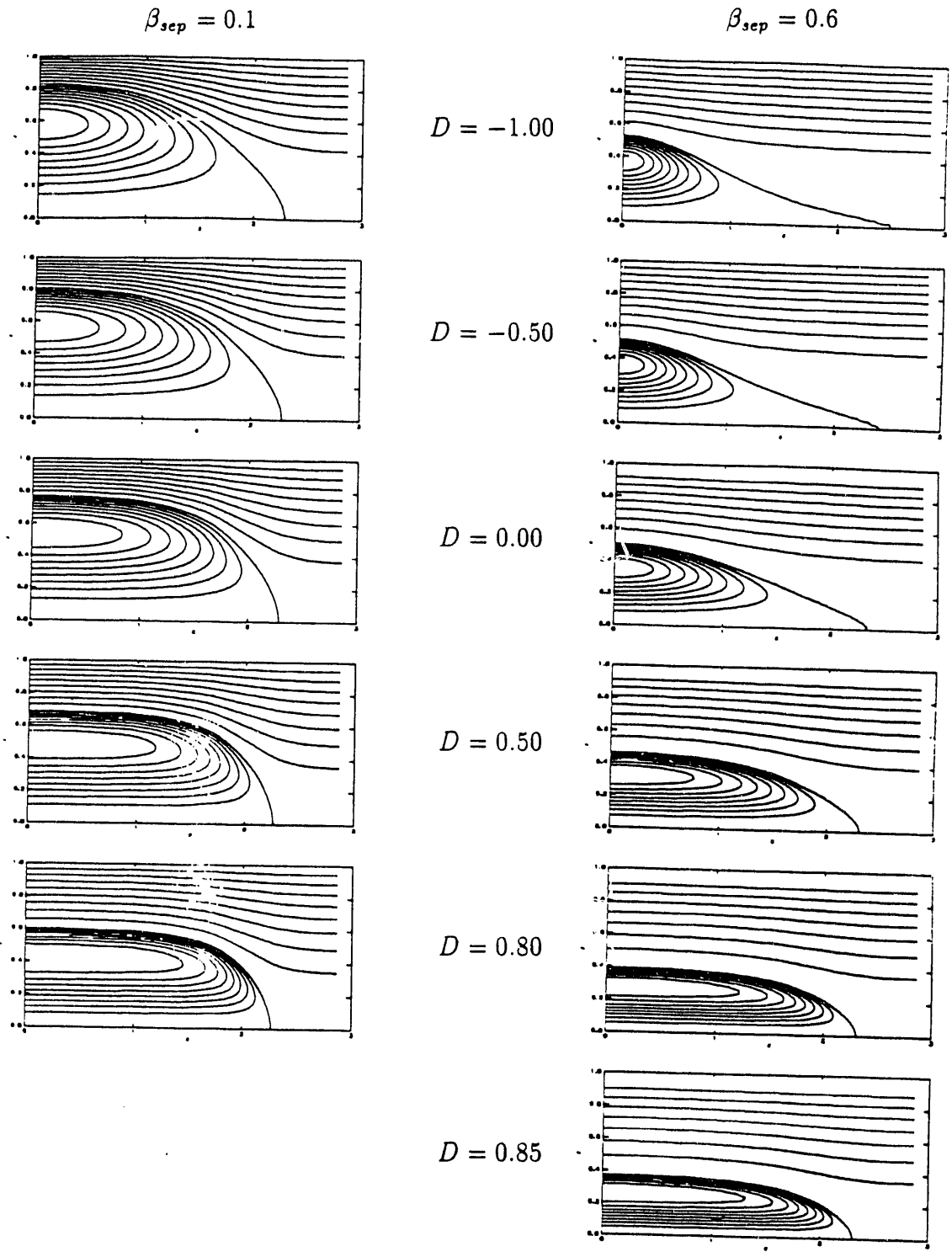

Figure 1. of 10
Cobb PF-19727

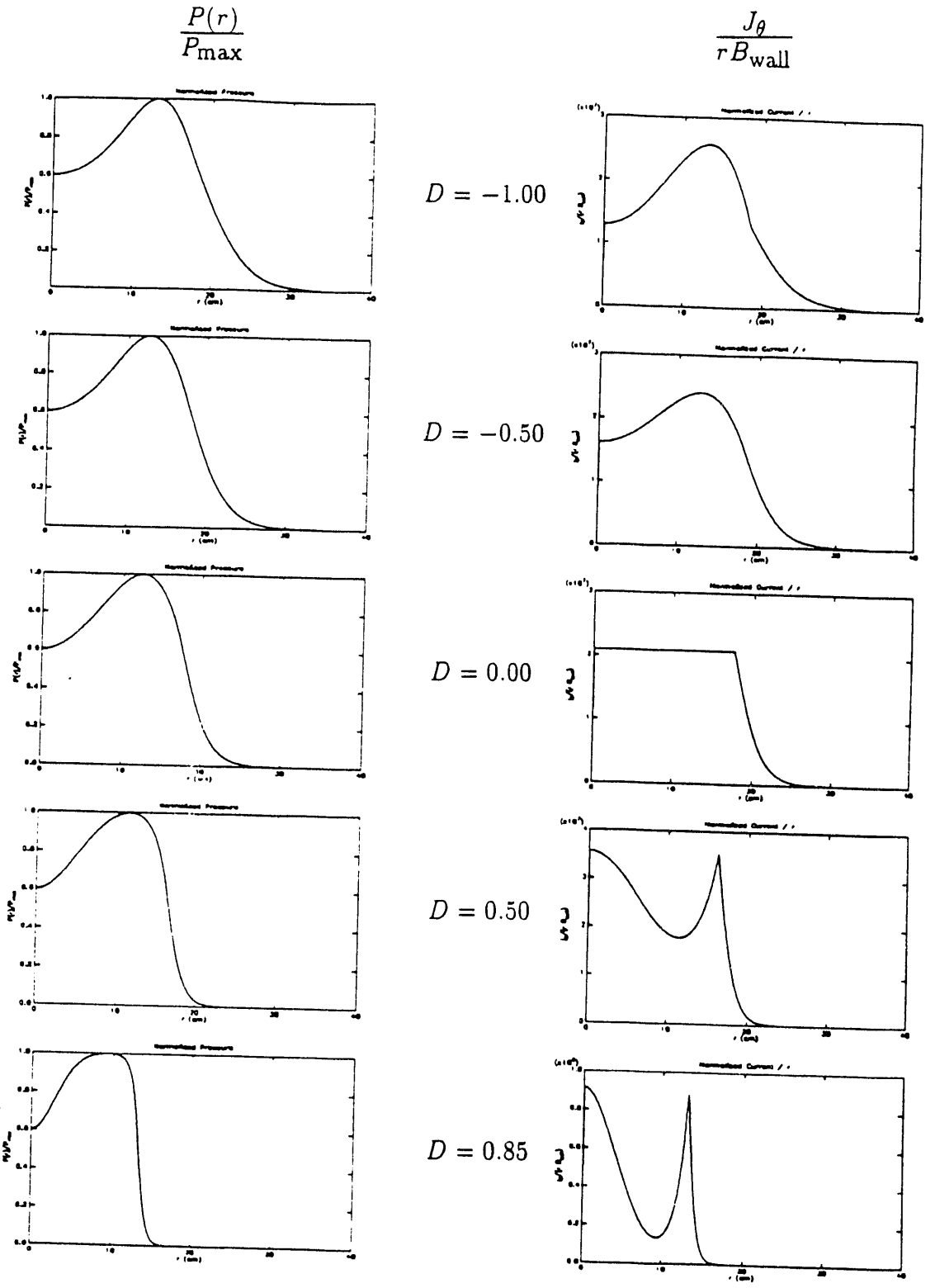

Figure 2. of 10
Cobb PF-19727

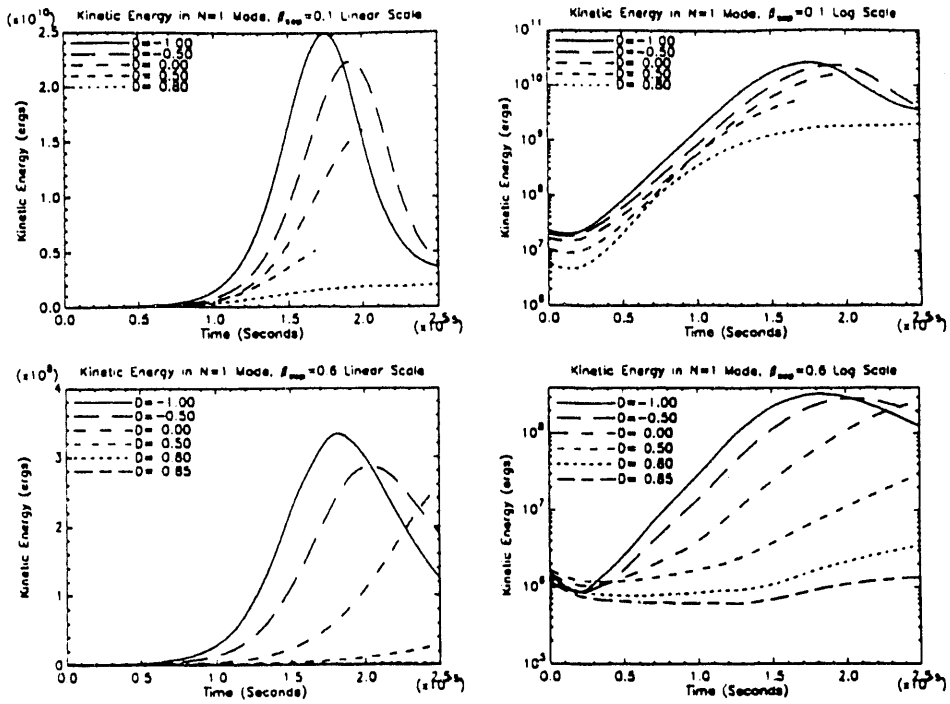

Figure 3. of 10
Cobb PF-19727

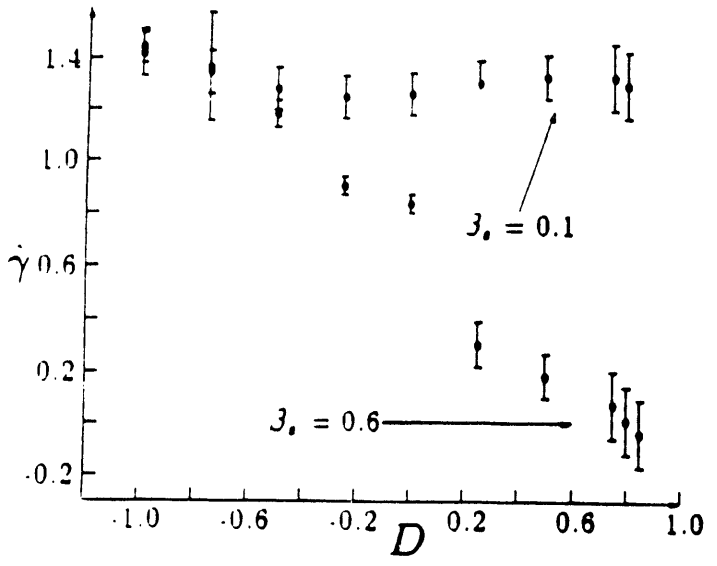

Fig. 4 of 10
Cobb PF-19727

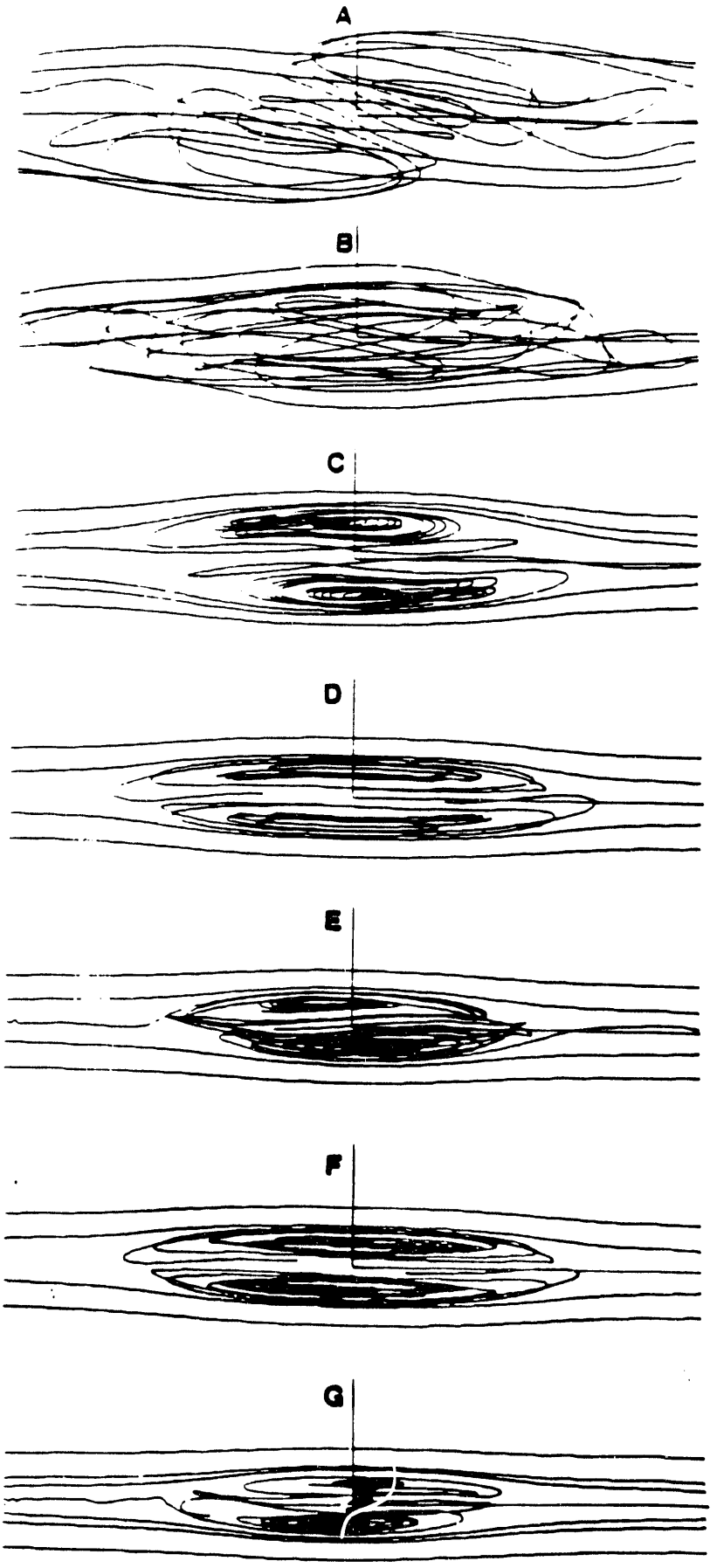

Fig. 5 of 10

Cobb PF-19727

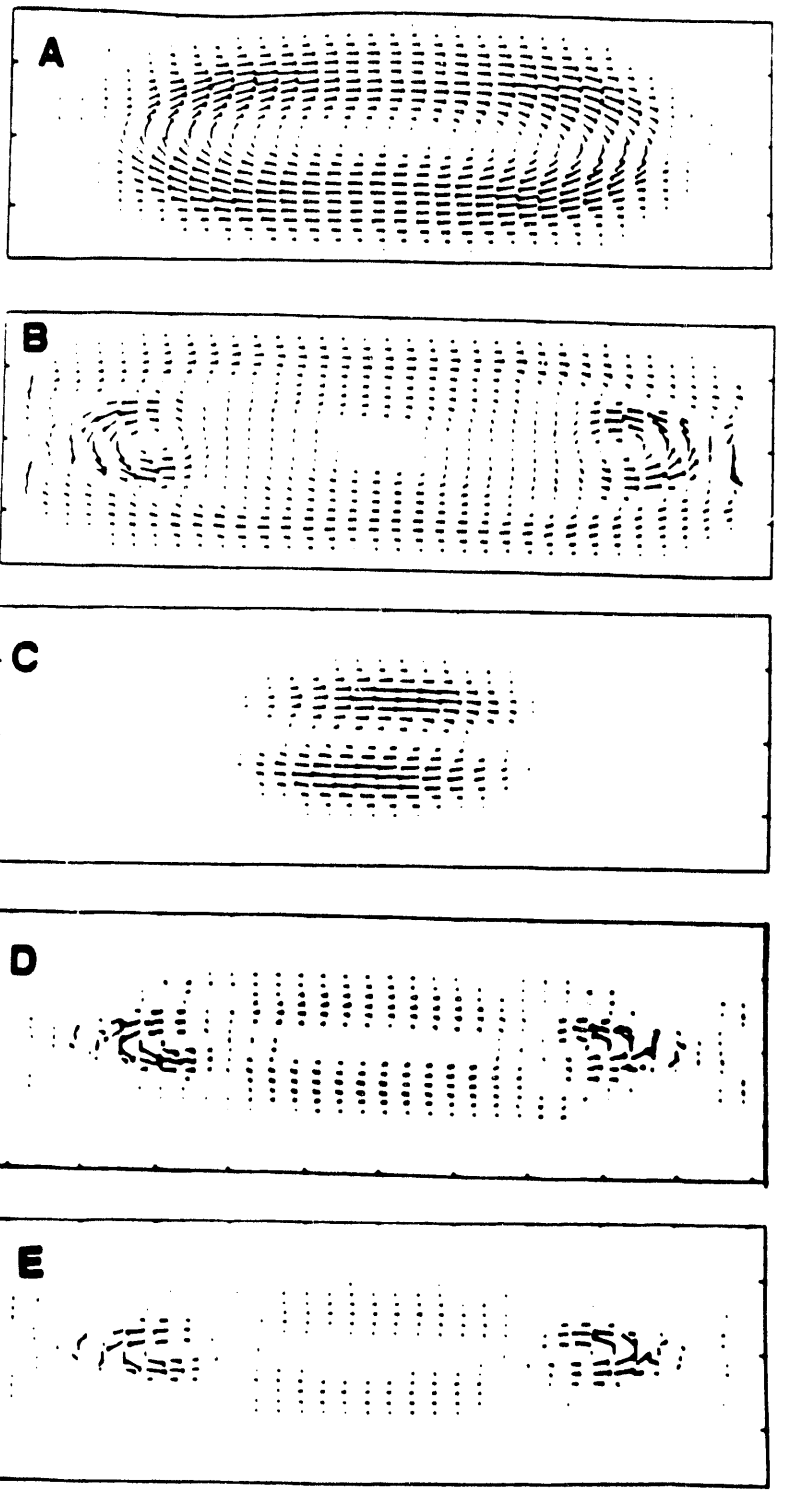

Fig. 6 of 10

Cobb PF-19727

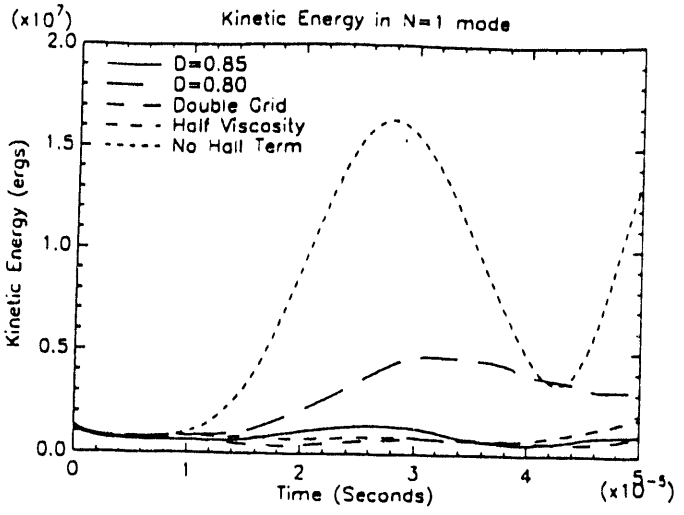

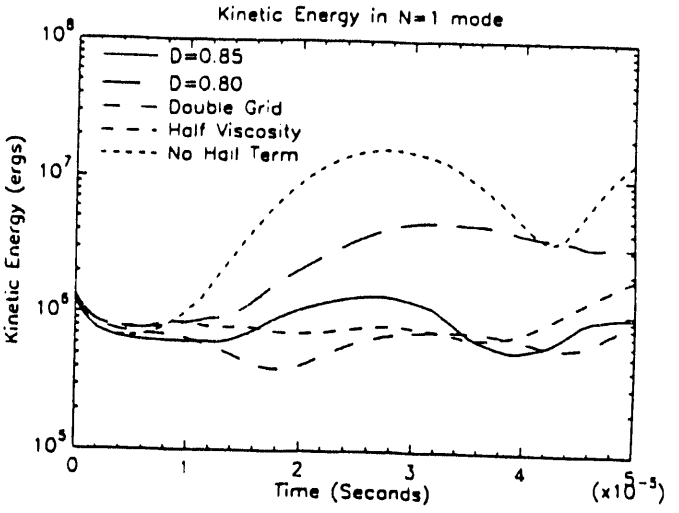

Figure 7. of 10
Cobb PF-19727

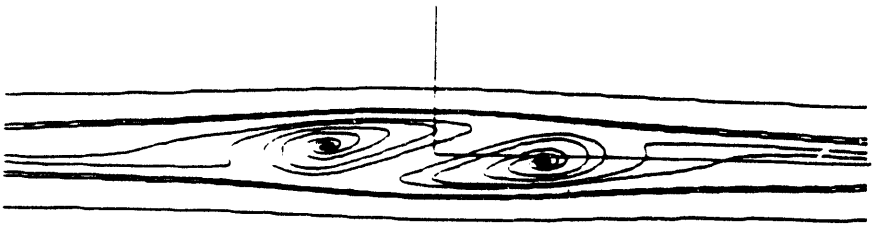

Fig. 8 of 10

Cobb PF-19727

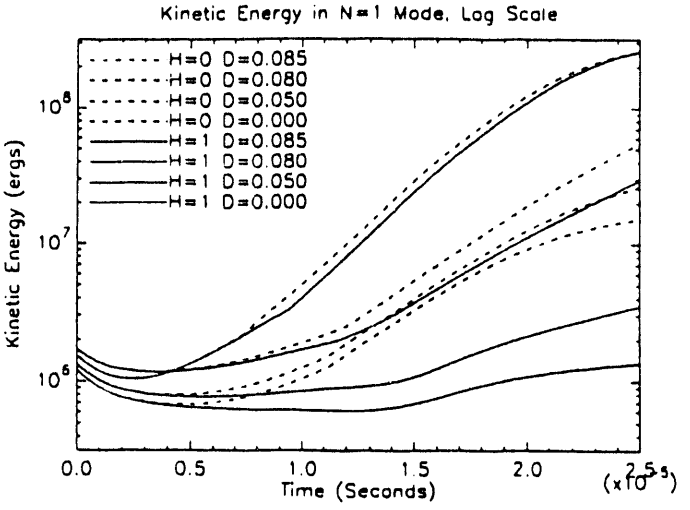

Figure 9. of 10
Cobb PF-19727

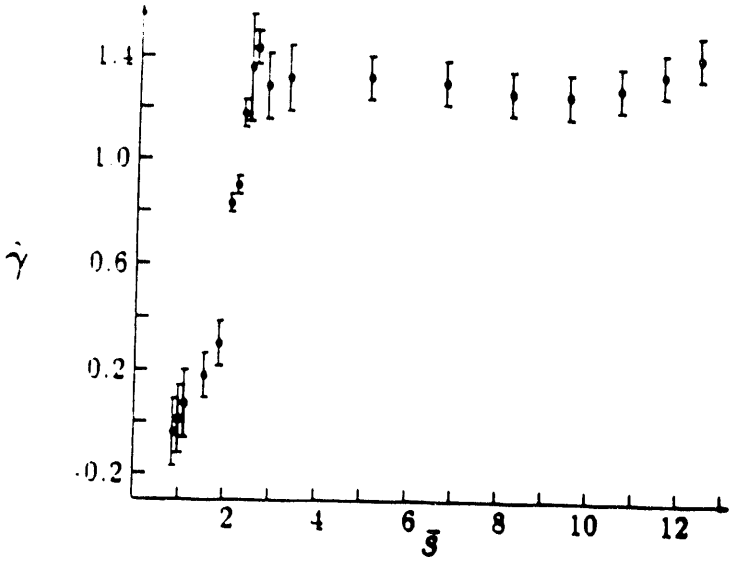

Fig. 10 of 10

Cobb PF-19727

END

DATE
FILMED
9/15/93